Structural and Electrical Properties of Some Sodium Phosphate Glasses Containing up to 35 mol% By-Pass Cement Dust

A.M. Abdel-Ghany [1], A.A. Bendary [2], T.Z. Abou-Elnasr [2], M.Y. Hassaan [2] and A.G. Mostafa [2]*

[1.] Basic Science Department., Faculty of Engineering Science, Sinai University, El-Arish, Egypt
[2.] Physics Department, Faculty of Science, Al-Azhar University, Nasr City, Cairo, Egypt
*drahmedgamal@yahoo.com

Abstract: By-pass cement dust (BCD) accumulates in huge amounts and attacks directly the human respiratory system. Thus, it has to be recycled in order to feel save environment. However BCD was used to prepare the following glasses, (70-x) mol% P_2O_5 -x mol% BCD -30 mol% Na_2O, [where $15 \leq x \leq 35$]. It was found that it is possible to prepare pure transparent glasses containing up to 35 mol% BCD. The obtained glasses were investigated from the structural and electrical points of view. It can be stated that the gradual increase of BCD in the glass batches act to increase the Q^2 and Q^1 speeches in the glass networks. It was found also that all glasses behave like semiconductor exhibiting Debye type relaxation. The anomaly observed in the conductivity dependence BCD content can be interpreted on the basis of mixed alkali and mixed alkali-alkaline earth effects and the change in Q^n speeches.

[Abdel-Ghany AM, Bendary AA, Abou-Elnasr TZ, Hassaan MY and Mostafa AG. **Structural and Electrical Properties of Some Sodium Phosphate Glasses Containing up to 35 mol% By-Pass Cement Dust**. *Nat Sci* 2014;12(8):146-153]. (ISSN: 1545-0740). http://www.sciencepub.net/nature. 20

Keywords: Phosphate Glasses; By-pass Cement Dust; Infrared Analysis; Electrical Transport Properties

1. Introduction

The accumulation of industrial wastes in huge amounts throughout the world becomes now a matter of interest. These wastes are usually produced in approximately all factories as by-products, and they cause mostly great harm to mankind everywhere. Among all these wastes by-pass cement dust (BCD) is of the highest dangerous effect, since it attacks directly the human respiratory system. However such like waste have to be recycled in order to feel safe environment.

On the other hand, phosphate glasses appeared of interest because they have higher thermal expansion coefficients, lower transition temperatures, interesting optical properties and high electrical conductivity [1]. Also these glasses possess the ability to accommodate high concentrations of transition metal ions and remain amorphous. In addition, phosphate glasses have a range of compositional and structural possibilities (ultra-, meta-, pyro-, and ortho-phosphates) that facilitate tailoring different chemical and physical properties [2, 3]. They have also considerable applications in optical transmission, solid state batteries, sensing laser technologies, and even extend to be host media for encapsulating radioactive wastes [4, 5].

During a certain program in our lab., for recycling some industrial wastes, BCD has been under focus now, and in a previous study the electrical transport properties of some sodium silicate glasses containing different proportions of BCD were thoroughly investigated. According to this study, it was concluded that BCD can be introduced up to 35 mol% into sodium silicate glasses and these glasses behave like semiconductors exhibiting Debye relaxation phenomenon [6].

However, in this article a trial will be done to prepare some phosphate glasses containing various additives, as high as possible, of BCD. The obtained pure amorphous glass samples will be investigated from the structural and electrical properties points of view, aiming to offer some glasses with different applications in the field of manufacturing amorphous semiconducting devices.

2. Experimental

The chemical composition of the used BCD is exhibited in Table (1).

The glass batches were prepared to supply glass samples having the following composition, [(70-x) mol% P_2O_5 -x mol% BCD -30 mol% Na_2O, (where $15 \leq x \leq 35$)]. The batches were melted in porcelain crucibles in an electric muffle furnace for 2 hrs at 1450 K. The obtained solid samples were then annealed at 520 K overnight. The visual examination of the obtained solids showed that all samples are of amorphous nature and they are also transparent.

The IR spectra of the studied glasses were obtained, using FTIR- Berken Elmer spectrometer; model RTX, in the range from 4000 to 400 cm^{-1}, applying KBr disk technique.

For electrical measurements, the obtained glasses were coated with an air drying silver paste to achieve good electrical contact. The measurements

were carried out using a computerized Stanford LCR bridge model SR 720 at four fixed frequencies [0.12,1, 10, 100 kHz], in the temperature range from 300 to 600 K.

Detailed information about BCD, method of preparation and measuring techniques are found in ref. (6).

Table 1. The obtained chemical composition of BCD

Constituents	CaO	SiO_2	Al_2O_3	K_2O	Cl^-	Fe_2O_3	Na_2O	MgO	SO_3	LOI*
Mass (%)	60.12	17.06	4.64	4.81	2.9	2.46	1.59	1.2	0.95	4.27

*LOI (Loss of ignition).

3. Results and Discussion

It is of interest to take a look about the internal structure of the studied glasses, which can help to discuss the observed changes in the measured properties. Therefore, the IR absorbance spectra were recorded at RT, between 400 and 4000 cm^{-1}, and they are presented in Fig. (1).

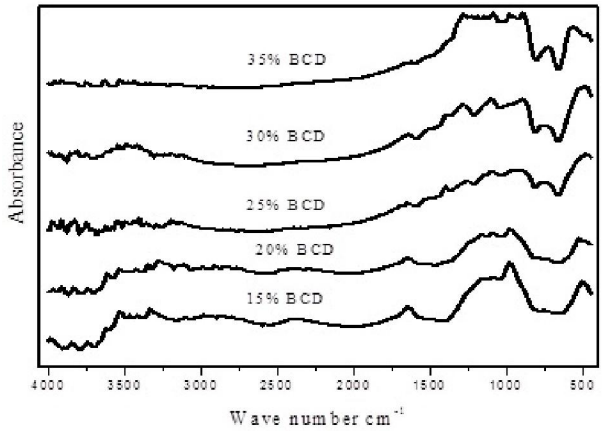

Figure 1. The as measured IR spectra of the studied glasses

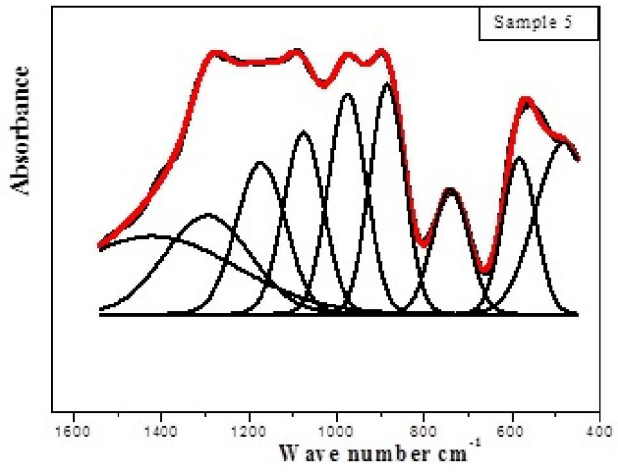

Figure 2. The de-convoluted IR spectrum of sample no. (5), as representative figure.

Considering the obtained spectra, it is observed that, the range of interest is in between 400 to 1600 cm^{-1} only, and in such range, the de-convolution program has been applied, in order to inspect as really as possible the functional groups in the glass network. Fig. (2) shows the de-convoluted spectrum of sample no. (5), as a representative figure, in the range from 400 to 1600 cm^{-1}.

From this figure, major deconvoluted bands are obviously appeared approximately in all glasses. These bands can be attributed to the vibration of some groups and bonds in the glass networks, which can be discussed as follows:

(1) A band appeared between 440 and 480 cm^{-1} in the spectra of all samples except sample no. (1), (that contains 15 mol% BCD). This band can be assigned to the symmetric bending vibration of Si–O–Si in SiO_2 tetrahedral [7]. The disappearance of this band in the first sample may be due to the poor SiO_2 content in this sample (about 2.5 mol %).

(2) The band appeared in between 500 and 580 cm^{-1} can be assigned to the presence of P–O bonds in PO_4 tetrahedral [8].

(3) The band appeared in the range from 740 to 770 cm^{-1}, in the obtained spectra of all glasses can be attributed to the symmetric stretching vibration of P-O-P bond in Q^1 speeches [9].

(4) The band appeared in between 880 and 900 cm^{-1}, can be assigned to the asymmetric stretching vibration of P-O-P bond in Q^1 speeches [10]. It is observed that the bands $(P\text{-}O\text{-}P)_s$ and $(P\text{-}O\text{-}P)_{as}$ shifted to higher frequency, which can be attributed to the changes in the phosphate chain length as well as the change of P–O–P bond angles, these angles depend on the characteristics of the metal cations in phosphate network [11-13].

(5) The band appeared around (975) cm^{-1}, can be assigned to the PO_3 vibration and/or the vibration of $(PO_4)^{3-}$ structural group in Q^o speeches [14, 15].

(6) The band appeared between 1074 and 1110) cm^{-1}, can be assigned to the symmetric stretching

vibration of PO_2 as well as the vibration of $(P-O)^-$ groups in Q^o speeches [16].

(7) The band appeared around 1170 cm^{-1} can be correlated to the vibration of two non-bridge oxygen (NBO) atoms bonded to a single phosphorus atom in PO_2 unit (O-P-O) [17].

(8) The band appeared from 1240 to 1300 cm^{-1}, can be correlated to the symmetric stretching vibration of two NBO atoms bonded to a phosphorus atom in PO_2 unit (O-P-O) and / or the O=P in Q^2 units [17].

(9) The band appeared in the range from 1334 to 1471 cm^{-1}, can be assigned to the asymmetric stretching vibration modes of the NBO atoms bonded to phosphorus atom and/or the vibration of P=O bond in Q^2 speeches [10].

(10) The band appeared between 1560 and 1600 cm^{-1}, can be assigned to the vibration of the present molecular water or hydroxyl-related bonds [18].

According to the IR results it can be stated that different phosphate speeches appeared in these glasses, since phosphorous forms the major glass network former atoms. As the BCD was introduced, some silicate groups appeared in the spectra of all samples except the first one that contains the least amount of SiO_2. The relatively large CaO ratio act to increase the Q^2 and Q^1 speeches as well as to increase the NBO atoms. The appearance of some H_2O or OH groups may be due to the used KBr disk technique. It is appeared also that, as BCD was increased, the intensity of these bands decreased which indicated that the introduced CaO (the major constituent of the BCD, about 60 mol%) decreases the absorption of water and strengthening the prepared solid glasses.

From another point of view, the electrical properties will be now investigated and Fig. (3) shows the measured total conductivity as a function of the reciprocal of the absolute temperature for sample no. (5) as representative figure. It is observed from this figure that at low temperatures the ac conductivity is considerably higher than the dc conductivity and shows weak temperature dependence and strong frequency dispersion. But at high temperatures the total conductivity approach the dc conductivity values and it shows strong temperature dependence and week frequency dispersion. It is observed also that the dc conductivity shows mostly linear change with 1000/T at high temperatures, while below certain temperature it shows a slight deviation from linearity and the activation energy becomes temperature dependent. All other samples show similar behavior [19, 20].

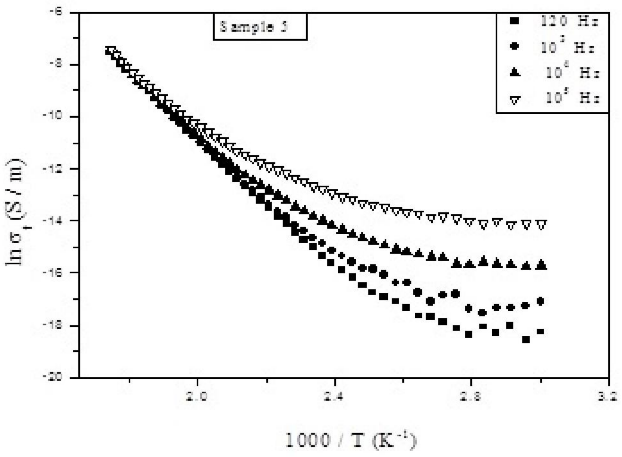

Figure 3. Total conductivity temperature dependence for sample no. (5), as a representative figure.

Figure (4), exhibits the change of ln σ_t as a function of BCD content, where it shows certain un-logic discontinuity. Inspecting this figure it can be regarded that when BCD (CaO) increased, the total conductivity decreased gradually until BCD reaches 25 mol%, where at this concentration, ln σ_t shows an increase until BCD reaches 30 mol%, where it shows little decrease again.

It is known that, the electrical conductivity below T_g can be determined mainly by the ionic radius of the introduced alkali or alkaline earth cations, since it affect directly the mobility of these cations. If two different alkali cations or if an alkali and an alkaline earth cations are introduced in a glass network, the total conductivity exhibits anomaly in its trend. It is known also that, with the increase of the difference between the ionic radii of both the present alkali and the alkaline earth cations, the electrical conductivity of these glasses decreased [21]. Respecting the observed change of ln σ_t of the studied glasses, it is supposed that, the first decrease of ln σ_t may be due to the introduced Ca^{2+} cations (BCD), which may housed in bridging oxygen position, possessing two positive charges. This was confirmed also from the obtained IR results, which showed a gradual increase of the Q^1 and Q^2 speeches as well as the NBO atoms. Due to the large ionic radius of Ca^{2+} cations, it acts to block the pathways of the mobile cations (Na^{2+}), and hence the mobility of Na^+ ions will be gradually reduced. With the gradual increase of BCD from 25 up to 30 mol%, the electrical conductivity increased, which may be due to the gradual increase of some metallic positive cations (such as Fe, Al, Mg and K). The presence of these cations may increase the electronic conductivity in this range of BCD content. At 30 mol% of BCD

and up, the conductivity showed little decrease again, which can be explained by considering that Ca^{2+} , Na+ and K+ cations are trapped in the glass networks, that is the ionic conductivity may be mostly stopped [22].

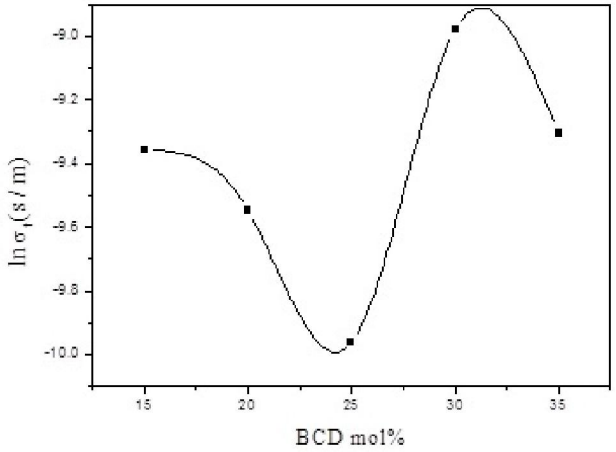

Figure 4. Total conductivity as a function of BCD content measured at 573 K

The dynamics of charge carriers in a glass network can be studied by considering Almond–West formula [23, 24], according to which the ac conductivity can be described by equation (1),

$$\sigma(\omega) = \sigma_{dc}\left(1 + \left(\frac{\omega}{\omega_H}\right)^n\right) \quad (1)$$

where σ_{dc} is the frequency independent conductivity, ω_H is the hopping frequency of the charge carriers and n is a dimensionless frequency exponent. The experimental conductivity data are fitted to equation (1) with σ_{dc} and ω_H as variables. The best fits to the conductivity spectra are exhibited by solid lines in Fig. (5) at different fixed temperatures, for sample no. 5 as representative figure . The values of n are given in Table (2) together with both W_H and σ_{dc}.

Table 2. The values of n, σ_{dc} and ω_H obtained from fitting with Almond–West formula

BCD mol%	n	ω_H (eV)	ln σ_{dc} (S / m)
15	0.87:0.17	0.18	-12.62
20	0.83:0.14	0.21	-14.58
25	0.49:0.03	0.26	-18.7
30	0.43:0.01	0.13	-11.36
35	0.59:0.01	0.24	-13.96

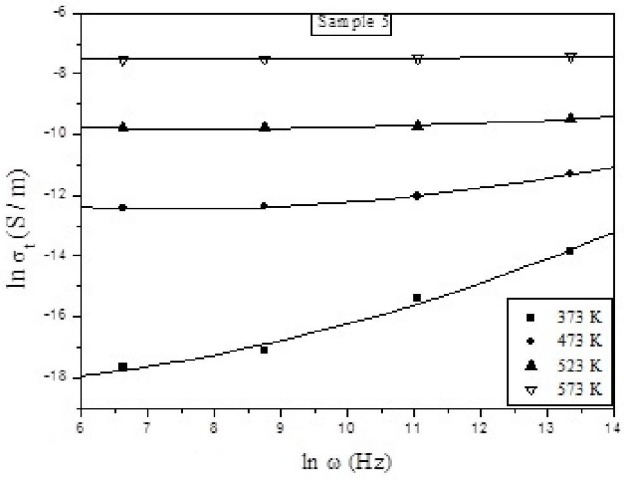

Figure 5. Experimental data (black points) and fitting (solid lines) according to Almond–West formula of ln σ_t varsus ln ω.

The activation energy of the dc conductivity can be calculated form the slopes of the obtained straight lines of the studied samples according to Arhenius equation (2),

$$\sigma_{dc}=\sigma_0 \exp(-\Delta E/kT) \quad (2)$$

where σ_0 is the pre-exponential factor and ΔE is the activation energy. From the slopes of the linear portion of the (ln σ_t ~ 1000/T) curves, the activation energy can be calculated. The variation of the activation energy with the variation of BCD is exhibited in Fig. (6), where it shows an opposite behavior to that of the total conductivity. This trend appeared to be a logic result.

The ac conductivity was found to obey the power law relation:

$$\sigma_{ac}(\omega) = A\omega^s \quad (3)$$

where σ_{ac} (ω) = is the ac conductivity, ω is the frequency, A is a weakly temperature dependent factor and **s** is the exponent factor. Different models based on reasonable physical assumptions emphasized the importance of this power law. The value of the exponent factor (**s**) can be calculated from the relation [**s** = d ln (σ)/d ln (ω)], and it is used to determine accurately the conduction mechanism. However, Fig. (7) represents the change of the factor **s** as a function of temperature for sample no. (5), as a representative figure, where it is appeared that **s** decreased gradually with temperature and its value was found to be slightly less than unity. It was found

also that all other samples represent similar behavior. Inspecting such variation and concerning the theoretical equations of the mostly applied models gives a primary indication about the conduction mechanism of the investigated glasses. It is noticed that the variation of **s** with T is compatible with that of the correlated barrier hopping (CBH) model, since this behavior gives the best fit for the obtained experimental data with equation (4),

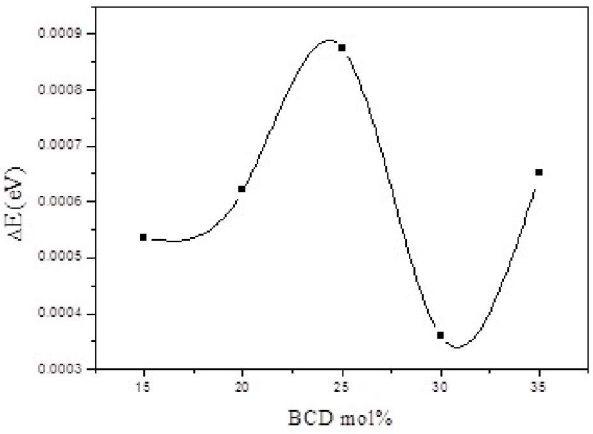

Figure 6. The dc activation energy of the dc conductivity as a function of BCD content.

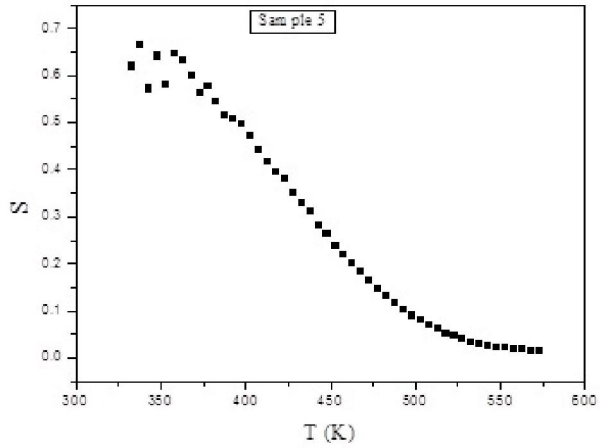

Figure 7. The change of s as versus temperature for sample no. (5), as representative figure.

The CBH model was early proposed by Pike [25] and was then modified by Elliott [26], where (s) can be explained by the theoretical equation (no. 4),

$$s = 1 - \frac{6\,kT}{W + kT \ln(\omega\tau_0)} \qquad (4)$$

Fig.s (8), (9) show the temperature dependence of the dielectric constant (ε') and the dielectric loss (ε'') respectively, for sample no. (5), as representative figures. The values of ε' and ε'' are almost temperature independent below 425 K and show weak frequency dispersion. Above this temperature, they show a strong temperature dependence as well as strong frequency dispersion. Such temperature was found to be constant for a given sample differs from one sample to another.

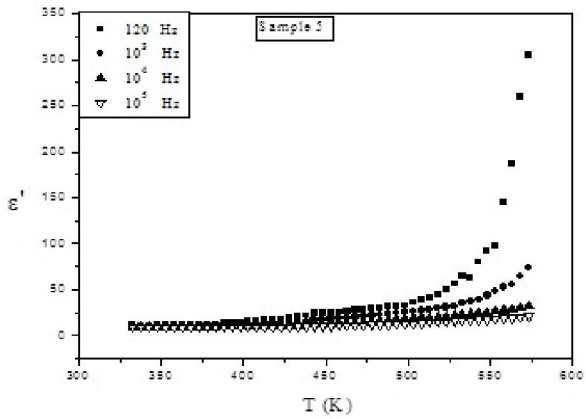

Figure 8. The dielectric constant temperature dependence for sample no. (5), as representative figure.

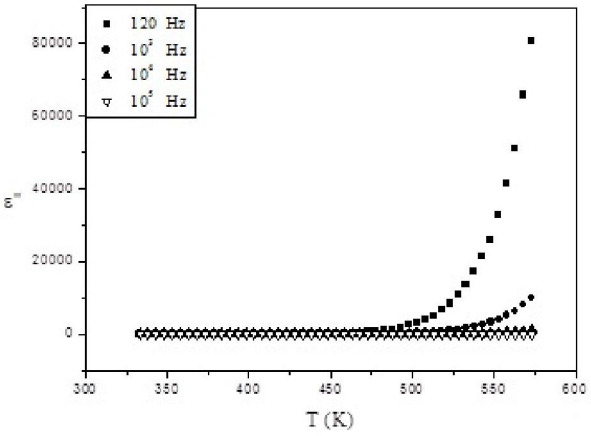

Figure 9. The dielectric loss temperature dependence, for sample no. (5), as representative figure.

Fig. (10) shows the variation of ε'' as a function of BCD mol%. Both the dielectric constant and the dielectric loss show the same behavior, and such behavior was found to be approximately similar to the behavior of the total conductivity, (see Fig. (4)) [27, 28].

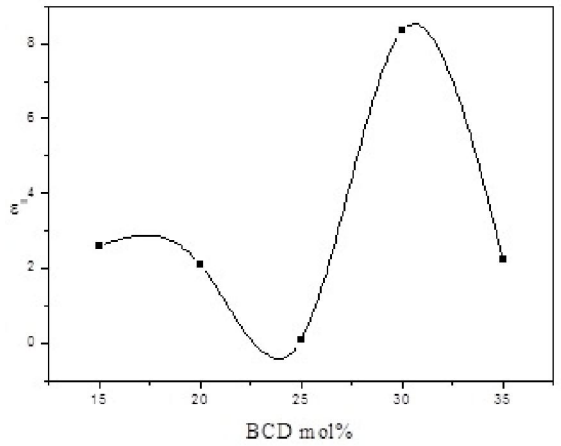

Figure 10. The dielectric constant versus the BCD mol%.

The dielectric loss factor (ε'') as a function of frequency was found to obey a power law of the form (equation 5) [29],

$$\varepsilon'' = B\,\omega^{m} \quad (5)$$

where B is a constant. The plot of ln (ε'') against ln (ω) must be a straight line with negative slope (m) as shown in Fig. (11), for sample no. (5), as a representative figure, at 323, 373, 408 and 473 K. The value of m as a function of temperature can be described by Guintini equation (equation 6) [29],

$$m = -4kT/W_m. \quad (6)$$

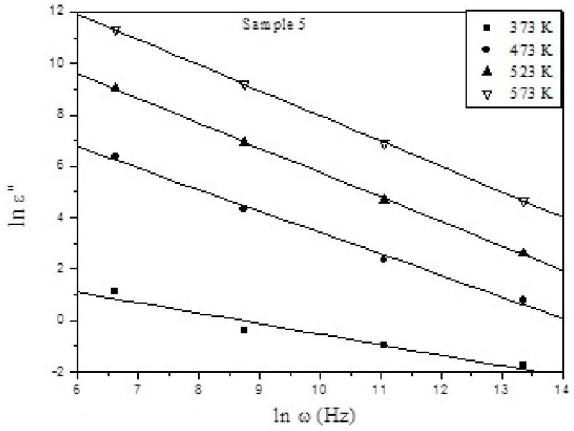

Figure 11. ln(ε'') versus ln(ω) at different fixed temperatures for sample no. (5), as a representative figure.

Figure (12) shows the variation of W_m as a function the BCD content, where the change of W_m shows an opposite behavior to that of the total conductivity ($\sigma_{(t)}$) [30, 31], which is also a logic result.

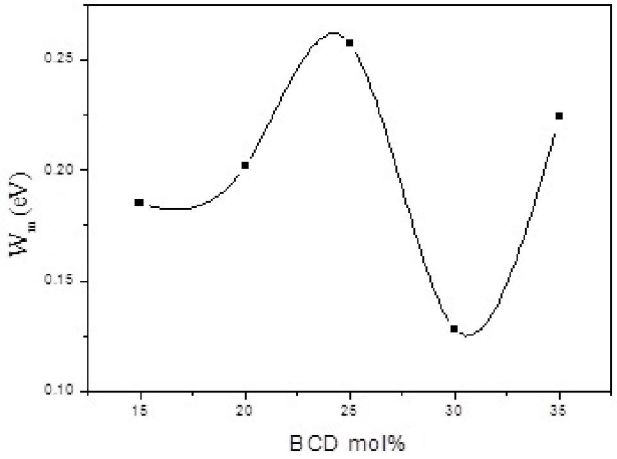

Figure 12. The variation of W_m as a function of BCD at fixed temperature.

Cole-Cole diagram (frequency dependence) and pseudo-Cole-Cole diagram (temperature dependence), for a complex dielectric data provides information about the various kinds of relaxation phenomena as well as the static and dynamic dielectric constants which are crucial values for device fabrication in micro-electronics. However both Cole-Cole diagrams were obtained by plotting the imaginary part of the electric modulus $M''(\omega)$ (equation (7)), against the real part $M'(\omega)$ (equation (8)), at constant temperature [32].

$$M''(\omega) = \varepsilon''/(\varepsilon'^2 + \varepsilon''^2) \quad (7)$$
$$M'(\omega) = \varepsilon'/(\varepsilon'^2 + \varepsilon''^2) \quad (8)$$

Figure (13) show Cole-Cole diagrams at 473 K for sample no.5, as representative figure, where it shows a single semicircle [32], and all samples exhibited similar behavior.

Figure (14) shows the pseudo Cole-Cole diagram at 100 kHz for sample no. (5), as a representative figure. It is clear that all plots of $M''(T) \sim M'(T)$ show a single semicircle, indicating a single relaxation process which agrees well with that predicted from Cole- Cole diagram.

In order to explain the obtained experimental data for the dielectric constant and loss, a symmetric distribution of relaxation times and dielectric loss can be conveniently obtained applying the following Cole - Cole equations (no. 9) [33],

$$\varepsilon''(\omega) = \frac{(\varepsilon_0 - \varepsilon_\infty)[(\omega\tau_d)^{(1-\alpha)}\cos(\alpha\pi/2)]}{[1 + 2(\omega\tau_d)^{(1-\alpha)}\sin(\alpha\pi/2) + (\omega\tau_d)^{2(1-\alpha)}]} \quad (9)$$

where ε_0 and ε_∞ are the static and high frequency dielectric constants, respectively, τ_d is the dielectric

relaxation time and α is an empirical distribution parameter having values between 0 and 1. The value of [α = zero] corresponds to a single relaxation time, i.e. Debye type relaxation. However, Fig. (15) shows the obtained experimental data for the ε'' (data point), where it has been fitted to those calculated from equation (9) (solid line). The parameters ε_0, ε_∞, τ_d and α are varied to get the best fits at different frequencies and temperatures. It is noticed that the fits are quite reasonable, and the factor α vary from 0.031 to 0.049 (Table 3) with a tendency to increase with the decrease of temperature and it shows little variation with composition. Such values represent a symmetric distribution of relaxation time for each sample.

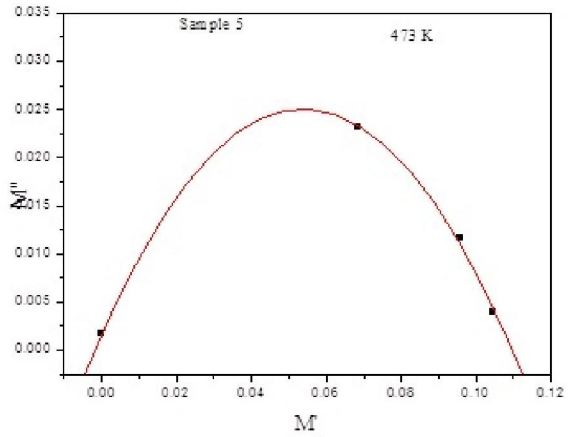

Figure 13. Cole-Cole diagram for sample no. (5), as a representative figure

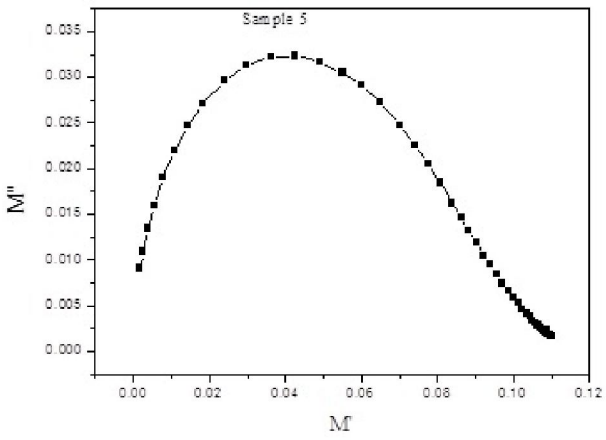

Figure 14. Pseudo Cole-Cole diagram at 100 k Hz for sample no. (5), as a representative figure.

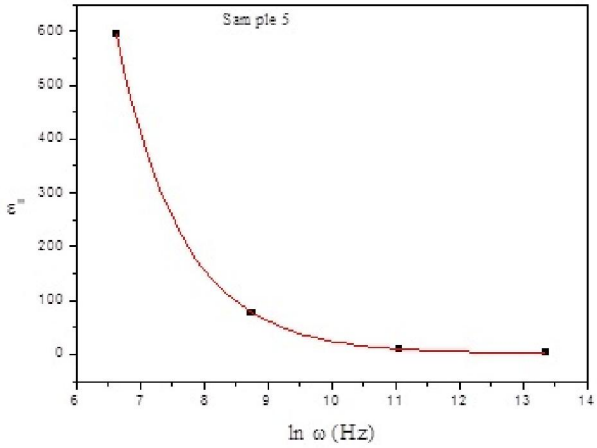

Figure 15. The fitting of ε" values with Cole-Cole equation, for sample no. (5), as a representative figure.

Table 3. The obtained values of **α** at 373 K for the studied samples.

BCD conc. %	α
15	0.042
20	0.038
25	0.049
30	0.031
35	0.042

4. Conclusion

BCD is a dangerous by-product and it is usually accompanying the production of cement. However, in this study, BCD was successfully introduced into some sodium phosphate glass batches up to 35 mol%., to prepare glasses for different applications. It was concluded that the gradual increase of BCD increases the strength of the obtained solid glasses and decreases the molecular water content, due to the increase of CaO (the major constituent of the BCD). This in turn may be due to the gradual increase of Q^1 and Q^2 speeches as well as the NBO atoms. The total conductivity measurements evidenced that all glasses behave like semiconductors, and the observed anomaly in the conductivity BCD content may be due to the coexistence of two different alkali cations (Na^+ and K^+) in addition to a large amount of an alkaline earth cation (Ca^{2+}). It was concluded also from the study of both cole-cole and pusido cole-cole diagrams that all glasses exhibit single relaxation process (Debye type relaxation).

Acknowledgement:

The authors would like to express their sincere gratitude to Eng./ Shaaban Saied and Eng./ Mohamed Kottb, the big mangers of El-Arish cement Co., for supplying the BCD used in this article.

Corresponding Author:
Prof. Dr. Ahmed G. Mostafa
Physics Department
Faculty of Science
Al-Azhar University, Nasr City, Cairo, Egypt
E-mail: drahmedgamal@yahoo.com

References

1. Y. M. Mustafa and A. El. Adawy, Phys. Status Solidi A, 179 (2000) 83.
2. E. Metwalli, M. Karabulut, D.L. Sideborton, M.M. Morsi and R.K. Brow, J. Non-Cryst. Solids, 344 (2004) 128.
3. G. D. Khattak, E.E. Khavaja, L.E. Wenge, D.J. Thompson, M.A. Said, A.B. Hallak and M.A. Daous, J. Non-Cryst. Solids, 194 (1990) 1.
4. A. G. Mostafa, M. Y. Hassaan, A. B. Ramadan, A. Z. Hussein and A. Y. Abdel-Haseib, J. Nature and Scieence, 5 (2013) 148.
5. H. A. Saudi, A. G. Mostafa, N. Shata, S. U. El-Kameesy and H. A. Sallam, J. Physica B, 406 (2011) 4001.
6. A. M. Abdel-Ghany, A. A. Bendary, T. Z. Abou-El-Nasr, M. Y. Hassaan and A. G. Mostafa, J. Nature and Scieence, 12(6) (2014) 139.
7. N. S. Hussain, M. A. Lopes and J. D. Santos, J. Materials Chemistry and Physics, 88 (2004) 5**.**
8. B. Qian Xiaofeng Liang, Shiyuan Yang, Shu He and Long Gao, J. Molecular Structure, 1027 (2012) 31.
9. A. M. Efimov, J. Non- Cryst. Solids, 209 (1997) 209
10. A. G. shikerkar, J. A.E. Desa, P. S. R.krishna and R. chitra, J. Non-Cryst. Solids, 270 (2000) 234.
11. J. C. Buyn, B. H. Kim, K. S. Hong, H. J. Jung, S. W. Lee and A. A. Lzyneev, J. Non-Cryst. Solids, 190 (1995) 288.
12. J. Koo, B. S. Bae and H. K. Na, J. Non-Cryst. Solids, 212 (1997) 193.
13. G. B. Rouse Jr., P.J. Miller and W. M. Risen, J. Non-Cryst. Solids, 28 (1978) 193.
14. A. Rulmont, Eur. J. Solid Inorg. Chem., 40 (1980) 535.
15. C. Daynand and M. S. Graw, J. Mater. Sci., 31 (1996) 1945.
16. S.W. Martin, Eur. J-Solid Inorg. Chem., 28(1) (1991) 163.
17. L. Baia, D. Muresan, M. Baia, J. Popp and S. Simon, Vib. Spectrosc., 43 (2007) 313- 318.
18. S. A. MacDonald, C. R. Schardt, D. J. Masiello and J. H. Simmons, J. Non-Cryst. Solids, 275 (2000) 72.
19. M. P. F. Graca, M. G. Ferreira da Silva and M. A. Valente, J. Eur. Cer. Soc., 28 (2008) 1197.
20. C. Kim, Y. Hwang, H.K. Kim, J.N. Kim, Phys. Chem. Glasses, 44 (2) (2003) 166.
21. F. M. Ezz Eldin and N. A. El Alaily, Materials Chemistry and Physics, 52 (1998) 175.
22. S. N. Salman and H. A. El-Batal, J. Non-Cryst. Solids, 168 (1994) 179.
23. D.P. Almond, A.R. West, Nature, 306 (1983) 453.
24. Alo Dutta, T. P. Sinha, P. Jena and S. Adak, J. Non-Cryst. Solids, 354 (2008) 3952.
25. G. E. PIKE, Phys. Rev. B, 6 (1972) 1572.
26. S. R. Elliott, Adv. Phys., 37 (1987) 135.
27. A. Ghosh and B. K. Chaudhuri, J. Mater. Sci., 22 (1987) 2369.
28. M. M. Elkholy, J. Mater. Sci., Mater. Electronics, 5 (1994) 157.
29. J. C. Giantini and J. V. Zancheha, J. Non-Cryst. Solids, 34 (1979) 419.
30. A. Mogus-Milankovic, B. Santic, C. S. Ray and D. E. Day, J. Non-Cryst. Solids, 263 & 264 (2000) 299.
31. A. S. Reo, Y. N. Ahammed, R. R. Reddy and T. V. R. Reo, J. Optics Materials, 10 (1998) 245.
32. K. S. Cole and R. S. Cole, J. Chem. Phys., 9 (1941) 341.
33. N. E. Hill, E. Vaughan, A. H. Price and M. Davies, "Dielectric Properties and Molecular Behavior" (London van Nostrand Reinhold Co.) 1969.

8/4/2014